On the implementation of the multiscale Hybrid High-Order method

Matteo Cicuttin, Alexandre Ern, Simon Lemaire

On the implementation of the multiscale Hybrid High-Order method

M. Cicuttin[1], A. Ern[1], and S. Lemaire[2]

[1] Université Paris-Est, CERMICS (ENPC), 6-8 avenue Blaise Pascal, 77455 Marne-la-Vallée Cedex 2, and Inria Paris, 75589 Paris, France
[2] École Polytechnique Fédérale de Lausanne (EPFL), FSB-MATH-ANMC, Station 8, 1015 Lausanne, Switzerland

Abstract The multiscale Hybrid High-Order method has been introduced recently to approximate elliptic problems with oscillatory coefficients. In this work, with a view toward implementation, we describe the general workflow of the method and we present one possible way for accurately approximating the oscillatory basis functions by means of a monoscale Hybrid High-Order method deployed on a fine-scale mesh in each cell of the coarse-scale mesh.

1 Introduction

Let Ω be an open, bounded, connected polytopal subset of $\mathbb{R}^d$, $d \in \{2,3\}$, with some characteristic length scale ℓ_Ω. We consider the model problem

$$\begin{cases} -\mathrm{div}(\mathbb{A}_\varepsilon \boldsymbol{\nabla} u_\varepsilon) = f & \text{in } \Omega, \\ u_\varepsilon = 0 & \text{on } \partial\Omega, \end{cases} \tag{1}$$

where $f \in L^2(\Omega)$ is non-oscillatory, and $\mathbb{A}_\varepsilon$ is an oscillatory, uniformly elliptic, bounded, symmetric matrix-valued field on Ω. The parameter $\varepsilon \ll \ell_\Omega$ encodes the fine-scale oscillations of the coefficients. An accurate, monoscale approximation of this problem would require an overwhelming number of degrees of freedom. In a multi-query context, where the solution is needed for a large number of right-hand sides, multiscale methods may be preferred. To this aim, different multiscale Finite Element Methods (msFEM) were proposed in the literature; we refer the reader to [8] for an overview. Other paradigms are also available to tackle multiscale problems, such as the Heterogeneous Multiscale Method (HMM) [1]. In the case of periodic coefficients, msFEM leads, on classical element shapes (e.g., simplices, quadrangles or hexahedra), in the lowest-order case, and without oversampling, to energy-error estimates of the form $(\sqrt{\varepsilon} + H + \sqrt{\varepsilon/H})$ where H represents the coarse-scale mesh-size (the regime of interest is $\varepsilon \le H \ll \ell_\Omega$). Higher-order extensions using simplical Lagrange elements of degree $k \ge 1$ were devised in [2], leading in the same setting of periodic coefficients to energy-error estimates of the form $(\sqrt{\varepsilon} + H^k + \sqrt{\varepsilon/H})$.

Recently the authors devised and analyzed a multiscale Hybrid High-Order (msHHO) method [3]. This method, which is a further development of

the monoscale HHO method introduced in [6] for diffusion problems and in [7] for linear elasticity, uses as discrete unknowns polynomials of degree $k \geq 0$ on the mesh faces and of degree $l \geq 0$ in the mesh cells. The crucial difference with respect to the monoscale HHO method is that the msHHO method uses oscillatory basis functions to define the local reconstruction operator, which is the core ingredient in building HHO methods. Two variants of the msHHO method were developed in [3], the mixed-order one ($l = k-1$, $k \geq 1$) and the equal-order one ($l = k$, $k \geq 0$). The motivations for considering HHO methods are that these methods support polytopal meshes, share a common design in any space dimension, are robust in various parametric regimes, and allow one to express basic conservation principles at the cell level, while offering computational efficiency since cell unknowns can be eliminated locally, leading to (compact-stencil) global problems with fewer unknowns. The monoscale HHO method has been bridged in [5] to the Hybridizable Discontinuous Galerkin (HDG) method and to the nonconforming Virtual Element Method (ncVEM). In the case of periodic coefficients, the msHHO method leads to energy-error estimates of the form $(\sqrt{\varepsilon}+H^{k+1}+\sqrt{\varepsilon/H})$. The msHHO method can be viewed as a higher-order, polytopal version of the msFEM à la Crouzeix–Raviart introduced in [10]. Other recent multiscale methods attaching discrete unknowns to the mesh faces include [9,11,12].

This contribution is organized as follows. In Section 2, we recall the oscillatory basis functions from [3] and discuss how they can be computed in each mesh cell. In Section 3, we outline the general workflow of the msHHO method. Finally, in Section 4, we present some numerical experiments illustrating how the accuracy in computing the oscillatory basis functions influences the accuracy of the msHHO method. For a detailed presentation of the implementation of the monoscale HHO method, we refer the reader to [4]. The present developments are part of the `Disk++` library, available as open-source under MPL license (`https://github.com/datafl4sh/diskpp`).

2 Oscillatory basis functions

Let $\mathcal{G}_\Omega := (\mathcal{T}_\Omega, \mathcal{F}_\Omega)$ be a coarse-scale mesh discretizing Ω, where $\mathcal{T}_\Omega$ and $\mathcal{F}_\Omega$ are, respectively, the collection of the mesh cells and faces. The oscillatory basis functions are defined on each mesh cell $T \in \mathcal{T}_\Omega$. Let $\mathcal{F}_{\partial T} := \{F_n\}_{0\leq n<m_T}$ be the collection of the faces composing the boundary of the mesh cell T. The purpose of the oscillatory basis functions is to provide a basis for the space

$$V_{\varepsilon,T}^{k+1} := \left\{ v_\varepsilon \in H^1(T) \mid \mathrm{div}(\mathbb{A}_\varepsilon \boldsymbol{\nabla} v_\varepsilon) \in \mathbb{P}_d^{k-1}(T),\, \mathbb{A}_\varepsilon \boldsymbol{\nabla} v_\varepsilon \cdot \boldsymbol{n}_T \in \mathbb{P}_{d-1}^k(\mathcal{F}_{\partial T}) \right\},$$

where $\boldsymbol{n}_T$ is the unit outward normal to T, $\mathbb{P}_d^{k-1}(T)$ is the space of d-variate polynomials of degree at most $(k-1)$ in T (with the convention that $\mathbb{P}_d^{-1}(T) = \{0\}$), and $\mathbb{P}_{d-1}^k(\mathcal{F}_{\partial T})$ is the space of piecewise $(d-1)$-variate polynomials of degree at most k on the faces of T. The superscript $(k+1)$ indicates that $V_{\varepsilon,T}^{k+1}$ has the same approximation capacity for smooth functions as the

polynomial space $\mathbb{P}_d^{k+1}(T)$. Letting $N_l^q := \dim(\mathbb{P}_l^q)$, the space $V_{\varepsilon,T}^{k+1}$ is of dimension $N_T^{k+1} := N_d^{k-1} + m_T N_{d-1}^k$.

2.1 Variational definition of the basis functions

There are N_d^{k-1} oscillatory basis functions attached to the mesh cell T. Let $\{\Phi_T^{k-1,i}\}_{0\le i<N_d^{k-1}}$ denote a basis of $\mathbb{P}_d^{k-1}(T)$ and let $\Lambda_{\mathcal{F}_{\partial T}}^k := \mathbb{P}_{d-1}^k(\mathcal{F}_{\partial T})$. Then, the oscillatory basis function $\varphi =: \varphi_{\varepsilon,T}^{k+1,i}$, for all $0 \le i < N_d^{k-1}$, is such that the pair $(\varphi, \lambda) \in H^1(T) \times \Lambda_{\mathcal{F}_{\partial T}}^k$ solves

$$\begin{cases} (\mathbb{A}_\varepsilon \boldsymbol{\nabla}\varphi, \boldsymbol{\nabla} w)_T + (\lambda, w)_{\partial T} = (\Phi_T^{k-1,i}, w)_T & \forall w \in H^1(T), \\ (\varphi, \mu)_{\partial T} = 0 & \forall \mu \in \Lambda_{\mathcal{F}_{\partial T}}^k. \end{cases} \tag{2}$$

Equivalently, φ is the unique minimizer in $H^1(T)$ of the energy functional $v_\varepsilon \mapsto \frac{1}{2}(\mathbb{A}_\varepsilon \boldsymbol{\nabla} v_\varepsilon, \boldsymbol{\nabla} v_\varepsilon)_T - (\Phi_T^{k-1,i}, v_\varepsilon)_T$ subjected to the constraint $(v_\varepsilon, \mu)_{\partial T} = 0$ for all $\mu \in \Lambda_{\mathcal{F}_{\partial T}}^k$.

There are $m_T N_{d-1}^k$ oscillatory basis functions attached to the boundary of T. Let $\{\Phi_{F_n}^{k,j}\}_{0\le j<N_{d-1}^k}$ denote a basis of $\mathbb{P}_{d-1}^k(F_n)$ for all $0 \le n < m_T$, and let us extend these functions by zero to the rest of ∂T. Then, the oscillatory basis function $\varphi =: \varphi_{\varepsilon,T}^{k+1,\delta(j,n)}$, with index $\delta(j,n) = N_d^{k-1} + nN_{d-1}^k + j$ for all $0 \le j < N_{d-1}^k$ and all $0 \le n < m_T$, is such that the pair $(\varphi, \lambda) \in H^1(T) \times \Lambda_{\mathcal{F}_{\partial T}}^k$ solves

$$\begin{cases} (\mathbb{A}_\varepsilon \boldsymbol{\nabla}\varphi, \boldsymbol{\nabla} w)_T + (\lambda, w)_{\partial T} = 0 & \forall w \in H^1(T), \\ (\varphi, \mu)_{\partial T} = (\Phi_{F_n}^{k,j}, \mu)_{\partial T} & \forall \mu \in \Lambda_{\mathcal{F}_{\partial T}}^k. \end{cases} \tag{3}$$

Equivalently, φ is the unique minimizer in $H^1(T)$ of the energy functional $v_\varepsilon \mapsto \frac{1}{2}(\mathbb{A}_\varepsilon \boldsymbol{\nabla} v_\varepsilon, \boldsymbol{\nabla} v_\varepsilon)_T$ subjected to the constraint $(v_\varepsilon, \mu)_{\partial T} = (\Phi_{F_n}^{k,j}, \mu)_{\partial T}$ for all $\mu \in \Lambda_{\mathcal{F}_{\partial T}}^k$. The variational problems (2) and (3) define the oscillatory basis functions $\{\varphi_{\varepsilon,T}^{k+1,i}\}_{0\le i<N_T^{k+1}}$.

2.2 Discretization and algebraic realization

The oscillatory basis functions defined by (2) and (3) cannot be computed explicitly, and one needs to approximate them by resorting to some discretization method. In this work, we use the monoscale HHO method. We start by submeshing the coarse-scale cell T by a fine-scale mesh $\mathcal{G}_T = (\mathcal{T}_T, \mathcal{F}_T)$, where $\mathcal{T}_T$ is the collection of the fine-scale cells composing $\mathcal{G}_T$ and $\mathcal{F}_T$ is the collection of the fine-scale faces. On the fine-scale mesh $\mathcal{G}_T$, we use the monoscale equal-order HHO method of degree $\kappa \ge 0$. Let $t \in \mathcal{T}_T$ be a fine-scale cell. We introduce the local space of discrete unknowns

$$\mathcal{U}_t^\kappa := \mathbb{P}_d^\kappa(t) \times \mathbb{P}_{d-1}^\kappa(\mathcal{F}_{\partial t}),$$

where $\mathbb{P}_d^\kappa(t)$ is the space of d-variate polynomials of degree at most κ on t and $\mathbb{P}_{d-1}^\kappa(\mathcal{F}_{\partial t})$ is the space of piecewise $(d-1)$-variate polynomials of degree at most κ on the faces of t which are collected in the set $\mathcal{F}_{\partial t}$. Following [6,7], the key ingredients of the monoscale HHO method are the local reconstruction operator $p_t^{\kappa+1} : \mathcal{U}_t^\kappa \to \mathbb{P}_d^{\kappa+1}(t)$ and the stabilization operator $s_t^{\kappa+1} : \mathcal{U}_t^\kappa \to \mathbb{P}_{d-1}^\kappa(\mathcal{F}_{\partial t})$ such that, for all $(v_t, v_{\partial t}) \in \mathcal{U}_t^\kappa$, we have for the reconstruction operator

$$(\boldsymbol{\nabla} p_t^{\kappa+1}(v_t, v_{\partial t}), \mathbb{A}_\varepsilon \boldsymbol{\nabla} q)_t := (\boldsymbol{\nabla} v_t, \mathbb{A}_\varepsilon \boldsymbol{\nabla} q)_t + (v_{\partial t} - v_{t|\partial t}, \mathbb{A}_\varepsilon \boldsymbol{\nabla} q \cdot \boldsymbol{n}_t)_{\partial t} \quad (4)$$

for all $q \in \mathbb{P}_d^{\kappa+1}(t)$, where $\boldsymbol{n}_t$ is the unit outward normal to t, together with the mean-value condition $(p_t^{\kappa+1}(v_t, v_{\partial t}), 1)_t = (v_t, 1)_t$, and for the stabilization operator, letting $p_t^{\kappa+1} := p_t^{\kappa+1}(v_t, v_{\partial t})$,

$$s_t^{\kappa+1}(v_t, v_{\partial t}) := \Pi_{\mathcal{F}_{\partial t}}^\kappa \Big(\big(v_{\partial t} - p_{t|\partial t}^{\kappa+1}\big) - \Pi_t^\kappa \big(v_t - p_t^{\kappa+1}\big)_{|\partial t} \Big), \quad (5)$$

where $\Pi_{\mathcal{F}_{\partial t}}^\kappa$ is the L^2-orthogonal projector onto $\mathbb{P}_{d-1}^\kappa(\mathcal{F}_{\partial t})$ and Π_t^κ is the L^2-orthogonal projector onto $\mathbb{P}_d^\kappa(t)$. The operators defined by (4) and (5) are used to build the local bilienar form $a_t : \mathcal{U}_t^\kappa \times \mathcal{U}_t^\kappa \to \mathbb{R}$ so that

$$\begin{aligned} a_t((u_t, u_{\partial t}), (v_t, v_{\partial t})) := {} & (\mathbb{A}_\varepsilon \boldsymbol{\nabla} p_t^{\kappa+1}(u_t, u_{\partial t}), \boldsymbol{\nabla} p_t^{\kappa+1}(v_t, v_{\partial t}))_t \\ & + (\eta_{\partial t} s_t^{\kappa+1}(u_t, u_{\partial t}), s_t^{\kappa+1}(v_t, v_{\partial t}))_{\partial t}, \end{aligned}$$

where $\eta_{\partial t}$ is a piecewise constant weighting coefficient on ∂t which is typically equal on each fine-scale face $f \in \mathcal{F}_{\partial t}$ to the maximum value of $\boldsymbol{n}_t \cdot \mathbb{A}_{\varepsilon|\partial t} \cdot \boldsymbol{n}_t$ on f divided by the diameter of f.

We are now ready to describe the discretization of (2) and (3) by the monoscale HHO method. Based on the fine-scale mesh $\mathcal{G}_T = (\mathcal{T}_T, \mathcal{F}_T)$ of the coarse-scale cell $T \in \mathcal{T}_\Omega$, we introduce the spaces

$$\mathcal{U}_{\mathcal{G}_T}^\kappa := \left\{ \bigtimes_{t \in \mathcal{T}_T} \mathbb{P}_d^\kappa(t) \right\} \times \left\{ \bigtimes_{f \in \mathcal{F}_T} \mathbb{P}_{d-1}^\kappa(f) \right\}, \qquad \mathcal{W}_T^{\kappa,k} := \mathcal{U}_{\mathcal{G}_T}^\kappa \times \Lambda_{\mathcal{F}_{\partial T}}^k.$$

For a pair $y = (y_{\mathcal{T}}, y_{\mathcal{F}}) \in \mathcal{U}_{\mathcal{G}_T}^\kappa$, we denote $(y_t, y_{\partial t}) \in \mathcal{U}_t^\kappa$ the local components attached to the fine-scale cell $t \in \mathcal{T}_T$, and we denote $y_{\partial T}$ the function defined on the boundary ∂T such that, for each fine-scale face $f \subset \partial T$, $y_{\partial T|f}$ is the component of $y_{\mathcal{F}}$ attached to the fine-scale face f. Note that $y_{\partial T}$ is generally not a member of the coarse-scale Lagrange multiplier space $\Lambda_{\mathcal{F}_{\partial T}}^k$ since it is a fine-scale piecewise polynomial. We define the bilinear form $a_{\mathcal{G}_T} : \mathcal{W}_T^{\kappa,k} \times \mathcal{W}_T^{\kappa,k} \to \mathbb{R}$ such that

$$a_{\mathcal{G}_T}((y, \lambda), (z, \mu)) := \sum_{t \in \mathcal{T}_T} a_t((y_t, y_{\partial t}), (z_t, z_{\partial t})) + (\lambda, z_{\partial T})_{\partial T} + (y_{\partial T}, \mu)_{\partial T}.$$

For all $0 \le i < N_T^{k+1}$, the oscillatory basis function $\varphi_{\varepsilon,T}^{k+1,i}$ is approximated by first finding the pair $(y^i, \lambda^i) \in \mathcal{W}_T^{\kappa,k}$ such that

$$a_{\mathcal{G}_T}((y^i, \lambda^i), (z, \mu)) = \Psi^i(z, \mu) \qquad \forall (z, \mu) \in \mathcal{W}_T^{\kappa,k},$$

where $\Psi^i(z,\mu) := (\Phi_T^{k-1,i}, z_T)_T$ for all $0 \le i < N_d^{k-1}$, and $\Psi^{\delta(j,n)}(z,\mu) := (\Phi_{F_n}^{k,j}, \mu)_{\partial T}$ for all $0 \le j < N_{d-1}^k$ and all $0 \le n < m_T$. Then, we set

$$\varphi_{\varepsilon,T|t}^{k+1,i} := p_t^{\kappa+1}(y_t^i, y_{\partial t}^i) \qquad \forall t \in \mathcal{T}_T, \quad \forall 0 \le i < N_T^{k+1}.$$

For each $0 \le i < N_T^{k+1}$, after static condensation, the global problem resulting from the above discretization is of size $N_{d-1}^\kappa \times \mathrm{card}(\mathcal{F}_T) + m_T N_{d-1}^k$, and has the following block-structure:

$$\begin{pmatrix} \left(\boldsymbol{A}_{\mathcal{F}\mathcal{F}} - \boldsymbol{A}_{\mathcal{F}\mathcal{T}}\boldsymbol{A}_{\mathcal{T}\mathcal{T}}^{-1}\boldsymbol{A}_{\mathcal{T}\mathcal{F}}\right) & \boldsymbol{B} \\ \boldsymbol{B}^\top & \boldsymbol{0} \end{pmatrix} \begin{pmatrix} \boldsymbol{y}_{\mathcal{F}}^i \\ \boldsymbol{\lambda}^i \end{pmatrix} = \begin{pmatrix} -\boldsymbol{A}_{\mathcal{F}\mathcal{T}}\boldsymbol{A}_{\mathcal{T}\mathcal{T}}^{-1}\boldsymbol{\Psi}_{\mathcal{T}}^i \\ \boldsymbol{\Psi}_\lambda^i \end{pmatrix}, \tag{6}$$

where the matrices $\boldsymbol{A}_{\mathcal{T}\mathcal{T}}$, $\boldsymbol{A}_{\mathcal{T}\mathcal{F}}$, $\boldsymbol{A}_{\mathcal{F}\mathcal{T}}$ and $\boldsymbol{A}_{\mathcal{F}\mathcal{F}}$ correspond to the monoscale HHO matrices for a diffusion problem (see [4]), whereas the matrices $\boldsymbol{B}$ and its transpose correspond to the imposition of the constraints by means of the Lagrange multipliers. The matrix $\boldsymbol{A}_{\mathcal{T}\mathcal{T}}$ is block-diagonal, with $\mathrm{card}(\mathcal{T}_T)$ blocks of size $N_d^\kappa \times N_d^\kappa$, hence it is invertible at no cost. Once (6) has been solved, one can recover $\boldsymbol{y}_{\mathcal{T}}^i = \boldsymbol{A}_{\mathcal{T}\mathcal{T}}^{-1}\left(\boldsymbol{\Psi}_{\mathcal{T}}^i - \boldsymbol{A}_{\mathcal{T}\mathcal{F}}\boldsymbol{y}_{\mathcal{F}}^i\right)$. A crucial observation is that the system matrix in (6) is independent of the index i enumerating the oscillatory basis function. Thus, a single matrix factorization followed by a multi-rhs solve is the procedure of choice.

Let us briefly describe the assembly of the matrix $\boldsymbol{B}$. Recall that the coarse-scale faces composing the boundary of T are enumerated as $\{F_n\}_{0\le n<m_T}$. Assume, for simplicity, that each coarse-scale face contains the same number, m_F, of fine-scale faces, and that the fine-scale faces in $\mathcal{F}_T$ are enumerated by counting first the fine-scale faces in F_0, then those in F_1, and so on until F_{m_T-1}, and finally all the fine-scale faces located inside T. Then we have $\bigcup_{0\le\beta<m_F} f_{nm_F+\beta} = F_n$ for all $0 \le n < m_T$. The matrix $\boldsymbol{B}$ has a block-structure composed of $\mathrm{card}(\mathcal{F}_T) \times m_T$ blocks, each block having size $N_{d-1}^\kappa \times N_{d-1}^k$. For all $0 \le \alpha < \mathrm{card}(\mathcal{F}_T)$ and $0 \le n < m_T$, the block $\boldsymbol{B}_{\alpha n}$ is zero whenever $\alpha < nm_F$ or $\alpha \ge (n+1)m_F$, otherwise we have

$$\boldsymbol{B}_{\alpha n, ij} = \int_{f_\alpha} \Phi_{f_\alpha}^{\kappa,i} \Phi_{F_n}^{k,j},$$

for all $0 \le i < N_{d-1}^\kappa$ and $0 \le j < N_{d-1}^k$, where $\{\Phi_{f_\alpha}^{\kappa,i}\}_{0\le i<N_{d-1}^\kappa}$ is a basis of the polynomial space $\mathbb{P}_{d-1}^\kappa(f_\alpha)$. The block-structure of the matrix $\boldsymbol{B}$ is illustrated in Figure 1 with $k=1$ and $\kappa=1$, so that each block is of size 2×2. The block-structure is composed of $\mathrm{card}(\mathcal{F}_T) = 9$ rows and $m_T = 3$ columns, and there are $m_F = 2$ nonzero blocks in each column.

3 General workflow of the msHHO method

The workflow of a simulation using the msHHO method involves two phases, an offline phase and an online phase. The offline phase is run first and consists, for each coarse-scale cell, in computing and storing the oscillatory basis

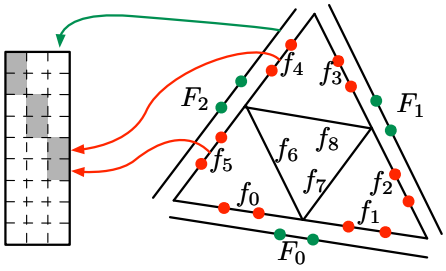

Figure1. Illustration of the block-structure of the matrix $\boldsymbol{B}$.

functions (cf. Sec. 2.2). During the offline phase, the multiscale reconstuction operator (plus, possibly, the coarse-scale stabilization operator) are also computed and stored, and the global system is assembled after local elimination of the cell unknowns. The offline phase can substantially benefit from parallel architectures. In the online phase, the computations done in the offline phase can be re-used as many times as needed to solve problems where, e.g., the source term is changed.

Let $T \in \mathcal{T}_\Omega$ be a coarse-scale cell. The local unknowns in the msHHO method belong to the space $U_T^{l,k} := \mathbb{P}_d^l(T) \times \mathbb{P}_{d-1}^k(\mathcal{F}_{\partial T})$, where $l = k-1$, $k \geq 1$ (mixed-order case) or $l = k \geq 0$ (equal-order case). The multiscale reconstruction operator $p_{\varepsilon,T}^{k+1} : U_T^{l,k} \to V_{\varepsilon,T}^{k+1}$ is defined so that, for all $(v_T, v_{\partial T}) \in U_T^{l,k}$, we have for all $q_\varepsilon \in V_{\varepsilon,T}^{k+1}$,

$$(\boldsymbol{\nabla} p_{\varepsilon,T}^{k+1}(v_T, v_{\partial T}), \mathbb{A}_\varepsilon \boldsymbol{\nabla} q_\varepsilon)_T := -(v_T, \operatorname{div}(\mathbb{A}_\varepsilon \boldsymbol{\nabla} q_\varepsilon))_T + (v_{\partial T}, \mathbb{A}_\varepsilon \boldsymbol{\nabla} q_\varepsilon \cdot \boldsymbol{n}_T)_{\partial T}, \tag{7}$$

together with the mean-value condition $(p_{\varepsilon,T}^{k+1}(v_T, v_{\partial T}), 1)_T = (v_T, 1)_T$. The implementation of the multiscale reconstruction operator $p_{\varepsilon,T}^{k+1}$ is almost identical to that of its monoscale version detailed in [4]; only three differences need to be noted. The first one is that in the multiscale case, the stiffness matrix is of size $N_T^{k+1} \times N_T^{k+1}$ (recall that $N_T^{k+1} = N_d^{k-1} + m_T N_{d-1}^k$) and is built using the gradients of the oscillatory basis functions (one needs to split the integral over T into a sum of integrals over $t \in \mathcal{T}_T$ so as to employ standard quadrature rules), whereas in the monoscale case, this matrix is of smaller size, namely $N_d^{k+1} \times N_d^{k+1}$, and is built using the gradients of polynomial basis functions. The second difference is that in the multiscale case, one uses the integrated form (7) of the rhs of (4), so as to take advantage of the fact that functions in $V_{\varepsilon,T}^{k+1}$ have (piecewise) polynomial divergence and flux. Finally, to enforce the above mean-value condition on $p_{\varepsilon,T}^{k+1}(v_T, v_{\partial T})$, one employs a Lagrange multiplier since the constant function is not directly accessible as one of the oscillatory basis functions (alternatively, one can find the decomposition of the constant function as a linear combination of the oscillatory basis functions). In the mixed-order case, the local bilinear form

$a_{\varepsilon,T} : U_T^{k-1,k} \times U_T^{k-1,k} \to \mathbb{R}$ is defined as

$$a_{\varepsilon,T}((u_T, u_{\partial T}), (v_T, v_{\partial T})) := (\mathbb{A}_\varepsilon \boldsymbol{\nabla} p_{\varepsilon,T}^{k+1}(u_T, u_{\partial T}), \boldsymbol{\nabla} p_{\varepsilon,T}^{k+1}(v_T, v_{\partial T}))_T,$$

and its implementation proceeds as in the monoscale case detailed in [4]. In the equal-order case, the local bilinear form $a_{\varepsilon,T} : U_T^{k,k} \times U_T^{k,k} \to \mathbb{R}$ is defined as

$$\begin{aligned} a_{\varepsilon,T}((u_T, u_{\partial T}), (v_T, v_{\partial T})) &:= (\mathbb{A}_\varepsilon \boldsymbol{\nabla} p_{\varepsilon,T}^{k+1}(u_T, u_{\partial T}), \boldsymbol{\nabla} p_{\varepsilon,T}^{k+1}(v_T, v_{\partial T}))_T \\ &\quad + (\eta_{\partial T}(u_T - \Pi_T^k(p_{\varepsilon,T}^{k+1}(u_T, u_{\partial T}))), v_T - \Pi_T^k(p_{\varepsilon,T}^{k+1}(v_T, v_{\partial T})))_{\partial T}, \end{aligned}$$

where the second term on the right-hand side is a coarse-scale stabilization with $\eta_{\partial T}$ being piecewise constant on ∂T and scaling on each face $F \in \mathcal{F}_{\partial T}$ as the maximum value of $\boldsymbol{n}_T \cdot \mathbb{A}_{\varepsilon|\partial T} \cdot \boldsymbol{n}_T$ on F divided by the diameter of F. For a mathematical discussion on this operator, we refer the reader to [3, Sec. 5.2], whereas its implementation proceeds as in the monoscale case detailed in [4]. The static condensation procedure and the assembly of the global system are then standard, and as in the monoscale HHO method. In any case ($l = k-1$ or $l = k$), the resulting global matrix has size $N_{d-1}^k \times \mathrm{card}(\mathcal{F}_\Omega)$.

Finally, the online phase, which is problem-dependent, consists in computing the right-hand side(s) and enforcing the boundary conditions. Dirichlet boundary conditions are enforced either by means of Lagrange multipliers or by zeroing out the degrees of freedom attached to the coarse-scale faces on the boundary of Ω.

4 Numerical experiments

In this section we briefly illustrate the msHHO method on the periodic test-case studied in [10]. We set $\Omega := (0,1)^2$, $f(x_1, x_2) := \sin(x_1)\sin(x_2)$, the (isotropic) oscillatory coefficient $\mathbb{A}_\varepsilon(x_1, x_2) := a(x_1/\varepsilon, x_2/\varepsilon)\mathbb{I}_2$ with $a(x, y) := 1 + 100\cos^2(\pi x)\sin^2(\pi y)$, and $\varepsilon = \pi/150 \approx 0.02$. We build a sequence of hierarchical triangular meshes of size $H_l = 0.43 \times 2^{-l}$ with $l \in \{0, \ldots, 9\}$; a reference solution is computed with the (equal-order) monoscale HHO method on the mesh of level $l_{\mathrm{ref}} = 9$ with polynomial degree $k_{\mathrm{ref}} = 2$. The left panel of Figure 2 presents relative energy-errors for the mixed-order msHHO method ($k = 2$) as a function of the coarse-scale meshsize for various resolutions of the oscillatory basis functions (fine-scale mesh corresponding to $l \in \{6, 7, 8\}$ and $\kappa \in \{0, 1\}$). We observe that insufficient resolution affects the quality of the multiscale numerical solution. The right panel presents the errors for the equal-order msHHO method of orders $k \in \{0, \ldots, 4\}$, the oscillatory basis functions being computed with $l = 8$ and $\kappa = 1$. The benefit of using a higher-order method is clearly visible up to $k = 3$, whereas for $k = 4$ the resolution of the reference solution (~ 50Mdofs) comes into play. Of particular interest is the regime for $k = 3$ where $H > \varepsilon$ and the error is below 10%.

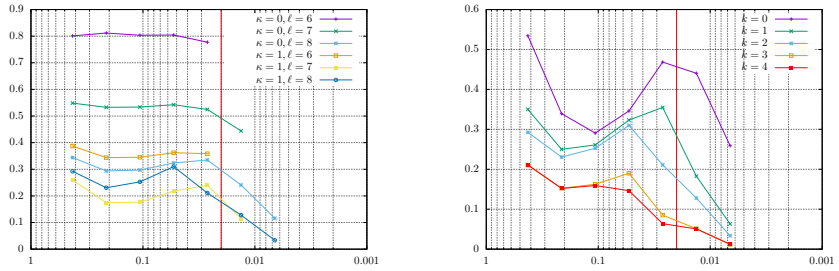

Figure2. Energy-error as a function of the coarse-scale meshsize for various resolutions of the oscillatory basis functions (left) and for various values of k. The vertical red line indicates the value of ε.

References

1. A. Abdulle, W. E, B. Engquist, and E. Vanden-Eijnden, *The Heterogeneous Multiscale Method*, Acta Numerica, 21:1–87, 2012.
2. G. Allaire and R. Brizzi, *A multiscale finite element method for numerical homogenization*, SIAM Multiscale Model. Simul., 4(3):790–812, 2005.
3. M. Cicuttin, A. Ern, and S. Lemaire, *A multiscale Hybrid High-Order method*, arXiv:1709.04679.
4. M. Cicuttin, D. A. Di Pietro, and A. Ern, *Implementation of Discontinuous Skeletal methods on arbitrary-dimensional, polytopal meshes using generic programming*, J. Comp. Appl. Math. (in press).
5. B. Cockburn, D. A. Di Pietro, and A. Ern, *Bridging the Hybrid High-Order and Hybridizable Discontinuous Galerkin methods*, ESAIM: Math. Model. Numer. Anal., 50(3):635–650, 2016.
6. D. A. Di Pietro, A. Ern, and S. Lemaire, *An arbitrary-order and compact-stencil discretization of diffusion on general meshes based on local reconstruction operators*, Comput. Meth. Appl. Math., 14(4):461–472, 2014.
7. D. A. Di Pietro and A. Ern, *A Hybrid High-Order locking-free method for linear elasticity on general meshes*, Comput. Meth. Appl. Mech. Engrg., 283:1–21, 2015.
8. Y. Efendiev and T. Y. Hou, *Multiscale Finite Element Methods - Theory and Applications*, volume 4 of Surveys and Tutorials in the Applied Mathematical Sciences. Springer-Verlag, New York, 2009.
9. Y. Efendiev, R. Lazarov, and K. Shi, *A multiscale HDG method for second order elliptic equations. Part I. Polynomial and homogenization-based multiscale spaces*, SIAM J. Numer. Anal., 53(1):342–369, 2015.
10. C. Le Bris, F. Legoll, and A. Lozinski, *MsFEM à la Crouzeix–Raviart for highly oscillatory elliptic problems*, Chinese Annals of Mathematics, Series B, 34(1):113–138, 2013.
11. L. Mu, J. Wang, and X. Ye, *A Weak Galerkin generalized multiscale finite element method*, J. Comp. Appl. Math., 305:68–81, 2016.
12. D. Paredes, F. Valentin, and H. M. Versieux, *On the robustness of Multiscale Hybrid-Mixed methods*, Math. Comp., 86:525–548, 2017.